Saliency Detection by Multiple-Instance Learning

Qi Wang, Yuan Yuan, *Senior Member, IEEE*, Pingkun Yan, *Senior Member, IEEE*, and Xuelong Li, *Fellow, IEEE*

***Abstract*—Saliency detection has been a hot topic in recent years. Its popularity is mainly because of its theoretical meaning for explaining human attention and applicable aims in segmentation, recognition, etc. Nevertheless, traditional algorithms are mostly based on unsupervised techniques, which have limited learning ability. The obtained saliency map is also inconsistent with many properties of human behavior. In order to overcome the challenges of inability and inconsistency, this paper presents a framework based on *multiple-instance learning*. Low-, mid-, and high-level features are incorporated in the detection procedure, and the learning ability enables it robust to noise. Experiments on a data set containing 1000 images demonstrate the effectiveness of the proposed framework. Its applicability is shown in the context of a seam carving application.**

***Index Terms*—Attention, computer vision, machine learning, multiple-instance learning (MIL), saliency, saliency map.**

I. Introduction

THE HUMAN visual system pays unequal attention to what is seen in the world. For instance, when looking at images in Fig. 1, people are usually attracted by some particular objects within them (i.e., flower, boat, and dog, respectively). Other subjects appear to be uninteresting for observers. This ability of "withdraw from some things in order to deal effectively with others" is called *attention* [1], [2].

Research on visual attention has found use in many applications, e.g., object recognition [3]–[6], image segmentation [7], [8], content-based retargeting [9], image retrieval [10], adaptive image display [11], and advertising design [12]. Because of these applications, extensive efforts from different disciplines have been spent toward visual attention, including computer vision [13]–[17], cognitive psychology [18], psychophysics [19], and neurobiology [20]. However, although the ability of selective attention seems to be natural to humans, the mechanisms behind this phenomenon are unclear. In this paper, one particular aspect of visual attention is explored from a computer vision viewpoint—*saliency detection*.

Manuscript received December 28, 2011; revised May 19, 2012; accepted July 29, 2012. Date of publication October 5, 2012; date of current version April 16, 2013. This work was supported in part by the National Basic Research Program of China (973 Program) under Grant 2011CB707104, by the National Natural Science Foundation of China under Grant 61172143, Grant 61105012, Grant 61072093, Grant 611721412, Grant 61125106, and Grant 91120302, by the Natural Science Foundation Research Project of Shaanxi Province under Grant 2012JM8024, and by the 50th China Postdoctoral Science Foundation under Grant 2011M501487. This paper was recommended by Associate Editor D. Goldgof.

The authors are with the Center for OPTical IMagery Analysis and Learning (OPTIMAL), State Key Laboratory of Transient Optics and Photonics, Xi'an Institute of Optics and Precision Mechanics, Chinese Academy of Sciences, 710119 Xi'an, China (e-mail: crabwq@opt.ac.cn; yuany@opt.ac.cn; pingkun.yan@opt.ac.cn; xuelong_li@opt.ac.cn).

Color versions of one or more of the figures in this paper are available online at http://ieeexplore.ieee.org.

Digital Object Identifier 10.1109/TSMCB.2012.2214210

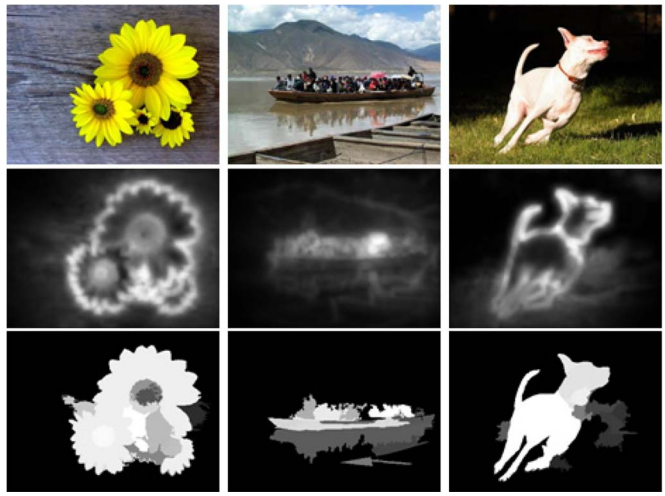

Fig. 1. Saliency detection. From top to bottom, each row represents the original images, the saliency maps calculated by CA [15], and the saliency maps calculated by the proposed framework, respectively.

The task of saliency detection is to extract the salient objects in an image, assuming that there is one or several salient ones within it. It is mainly approached by three steps, namely, *feature selection*, *saliency calculation*, and *map normalization*. First, low-level features, such as color, intensity, orientation, and motion, are selected as the basic elements for supporting saliency detection. Second, the saliency value for each pixel in an input image is calculated according to a predefined model. In the end, saliency maps from different sources are integrated and normalized to get a final result. The saliency value is generally denoted by a number scaled to [0, 1] and shown in a gray image. The greater value the pixel has, the higher possibility it is of being salient. A typical example of saliency detection results is illustrated in the middle row in Fig. 1.

Similar to existing algorithms, the general procedure for saliency detection is also followed in this paper; Unlike existing algorithms, it is conducted in a different framework, i.e., *multiple-instance learning* (MIL) [21].

A. Related Work

Algorithms for saliency detection can be generally categorized as *model based* and *computation based*.

- *Model-based* algorithms adopt a top-down route. In these algorithms, a high-level model is first established empirically. Then, the subsequent calculation is conducted with respect to the defined model. The work by Koch and Ullman [22] is among the earliest attempts of this kind. They proposed a bionics model to intimate an attention shift of human and primate. In their implementation, a neuron-like network is employed to combine several

topographical parallel saliency maps from different image clues. Then, a winner-take-all mechanism keeps the selective attention point drifting from one conspicuous location to another. Another architecture, probably the most influential one, is the work by Itti *et al.* [23]. Inspired by the early vision of primates, they extract multiscale features through a set of linear "center surround" operations. Then, the "focus of attention" is determined by combining and normalizing the across-scale maps. Based on this, Walther *et al.* [6] presented a combined model for spatial attention and object recognition, in which the entire visual field is considered but only part of it is sufficient for recognition. They report that the approach yields encouraging results and is biologically and applicably plausible.

Different from the aforementioned three biologically inspired models, Hou and Zhang [24] tackled the saliency problem from the spectral residual domain. Through a statistical and experimental analysis, they find that the log spectrum of natural images shares a similar trend whereby the regions corresponding to singular points in the statistical curves are responsible for the anomalous ones that count for saliency. In addition to that, there are still other algorithms treating this problem with machine learning approaches. Liu *et al.* [25] formulated saliency detection in a Markov random field (MRF) framework. Model parameters are learned on a labeled data set, and the static and sequential images are tested afterward to demonstrate its effectiveness. Judd *et al.* [26] dealt with saliency by a support vector machine (SVM), assuming that the saliency level can be determined by the distance to the decision boundary. Linear kernels are selected to train the involved parameters, and the results are evaluated on a data set containing 1003 eye tracking images.

- *Computation-based* algorithms, on the contrary, follow a bottom-up route. Saliency of this type is typically calculated by contrast from low-level features. For example, Wang and Li [27] proposed a two-stage approach to saliency detection. In the first stage, the spectrum residual model [24] is extended by introducing two modules, namely, automatic channel selection and decision reversal. In the second stage, incomplete salient regions are propagated based on the basic Gestalt grouping principles. Achanta *et al.* [16] presented an algorithm that outputs saliency maps with well-defined boundaries of salient objects, which are obtained by retaining more frequency content from the input image than previous techniques. They also constructed a data set containing labeled segmentation of 1000 images to be used as ground truth. Later, Radhakrishna and Sabine [28] detected saliency with respect to the hypothesis that the scale of an object relates to the image borders. They thus varied the bandwidth of the center surround-filtering near-image borders using symmetric surrounds to detect saliency. Zhang *et al.* [29] provided a Bayesian expression of the saliency task. Self-information and pointwise mutual information are fused to generate a final result. Harel and Koch [30] designed a graph-based algorithm consisting of two steps: 1) forming activation maps on certain feature channels and 2) combining them in a manner that highlights conspicuity. It is claimed that the model is mathematically simple and practically plausible. Cheng *et al.* [31] brought in a region-based concept that simultaneously evaluates global contrast difference and spatial coherence.

  In addition to various techniques involved in the detection procedure, there are other algorithms trying to get a novel definition for saliency. Goferman *et al.* [15] proposed a new type of saliency called context-aware saliency, which aims at extracting the image regions representing the scene, whereas previous definitions sought to identify fixation points or the dominant objects. Chang *et al.* [17] defined the salient region not only from the distinctiveness of a single image but also considering the repeatedness among images. Wang *et al.* [32] considered saliency as an anomaly with respect to a given context, which can be global or local. The global context is estimated in the whole image relative to a bunch of images. In the local context, the input image is partitioned into patches, and saliency in each patch is computed by contrast to other patches.

B. Limitations of Existing Algorithms

Although various algorithms for saliency detection have been presented in the past few years, and good performance for predicting human fixations in viewing images has been achieved in some circumstances, there are still limitations.

Lack of full resolution. The saliency maps of several algorithms suffer from low resolution. For example, the map by Itti *et al.* [23] is 256 times smaller than the original image, and the one by Hou and Zhang [24] is fixed by 64 pixels in width (or height). This will lead to a limited applicability in some situations, such as segmentation and recognition.

Inconsistency. Most existing algorithms generate inconsistent saliency maps, which is undesirable. Some of these have fuzzy maps with ill-defined boundaries. Some others highlight object boundaries but fail to detect the whole target region. There are still others emphasizing smaller salient regions other than the whole desired one. This inconsistency makes the detection task less fulfilled and limits the usefulness in certain applications.

The aforementioned two limitations are mainly derived from the following reasons.

First, not all image clues are utilized for supporting saliency calculation. Humans perceive the world not only by color but also by other types of clues such as texture, shape, depth, shadow, and motion. This rule of perceiving is true for visual attention processing [22]. Nevertheless, to the best of the authors' knowledge, color is probably the most frequently employed feature in existing work of saliency detection. In addition to that, motion and spectrum have been less explored in [16] and [33]. Other clues such as texture, boundary, shape, etc. are rarely considered.

Second, existing models have not well considered the learning ability of humans. Previous works are, in general, based on single image contrast. The consequently derived model is mostly heuristic. This makes the machine independent of

learning ability, to which the human attention is closely related. Recently, learning-based algorithms seem to be generating encouraging results. However, there are still problems to be solved. For example, saliency maps of Judd *et al.* [26] were learned from an SVM classifier. The data set employed in training is composed of images with ground-truth fixation points instead of regions. Sometimes, a few fixation points may be adequate to use. However, most of the time, the desired results are salient regions. Liu *et al.* [34] proposed to detect saliency by MRF. Although the involved parameters are learned from labeled images, no higher level features are incorporated. In addition, the training images are labeled with rectangles larger than the actual salient objects. This makes the model less accurate.

C. Proposed Framework

In this paper, a saliency detection framework based on MIL is presented. It is aimed to overcome the challenge that we do not know but have to detect the salient object in an input image.

First, different from existing techniques, the detection procedure is modeled as a MIL problem, where segmented regions are taken as *bags* and the sampled points within them as *instances*. Second, more features, including low-, mid-, and high-level, are incorporated into the learning and testing process. They are position, color, texture, scale, center prior, and boundary. Since humans recognize the world by integrated sources of data, the addition of other types of information, not only color and brightness, might be helpful. In the end, performance is evaluated on a data set of 1000 images with four MIL implementations.

The remainder of this paper is organized as follows: Section II formulates the saliency detection task as a MIL problem. Section III gives a detailed description of the distinctive features employed in the framework. Experimental results are shown in Section IV, and an image retargeting application is demonstrated in Section V. Section VI discusses several issues related to the proposed algorithm. Section VII concludes this paper.

II. Formulation

MIL is a kind of learning technique with incomplete knowledge about the labels of training examples. Unlike standard supervised learning, in which each training instance has a known label, the examples here are bags of instances. Each bag receives a single label, and the label of each instance is not necessarily known. A positive bag means that at least one instance in the bag is positive, whereas a negative bag indicates that all instances in the bag are negative. The objective of MIL is to classify unseen bags or instances based on the labeled bags in the training data.

Since the seminal work of Dietterich *et al.* [21], MIL has been researched a lot [35], [36]. Early work of this subject is mainly for the Boolean labeled problem. That means the learning result is either 0 or 1. After the introduction of real-valued labels [37], i.e., the label is in the range of [0, 1], MIL has achieved greater popularity in many applications. This is chiefly due to its tolerance to the ambiguity of the training data. For example, Viola *et al.* [38] claimed that object detection had inherent ambiguities for traditional supervised learning algorithms. For this reason, they adopt the use of MIL in their face detection algorithm. Babenko *et al.* [39] made an analogous argument and thus proposed to use a MIL-based model for object tracking.

In this paper, the question to be addressed is that we know there must be at least one salient object in the image, but we do not know exactly where it is. Therefore, saliency detection is explicitly acknowledged as an innate MIL problem. Existing learning-based algorithms [26], [34] tackle this problem pixel by pixel. In order to maintain the consistency of the resulting saliency maps, it is processed region by region instead. Each image is composed of tens of regions (bags), and each region consists of numerous pixels (instances). The bag's degree of being salient is determined according to its belonged instances. This is a typical MIL problem.

A. Definition

Traditional learning algorithms for estimating $p(y|x)$ require a training data set of the form $\{\langle x_1, y_1\rangle, \ldots, \langle x_n, y_n\rangle\}$, where x_i is an instance and $y_i \in \{0, 1\}$ is its binary label. In MIL, the training data can be denoted by $T = \{\langle B_1, \ell_1\rangle, \ldots, \langle B_b, \ell_b\rangle\}$, where B_i is a bag and ℓ_i is its corresponding binary label. Let B_{ij} be the jth instance of bag i and B_{ijk} the value of instance B_{ij} on feature k. By learning the correlation between bags and instances, a model can be obtained, according to which each instance in the testing data receives a real-valued label. The predicted label is defined as

$$\ell_i = \max_j(\ell_{ij}) \tag{1}$$

where ℓ_{ij} is the instance label, which is not known during training. In summary, the saliency detection problem is formulated as follows: *Given an image I, its corresponding bags and instances are first extracted. Then the classification model is learned by MIL. For a future testing image, its bag label is decided according to the obtained model.*

B. Learning Saliency Detection Model

Different techniques can be employed for MIL. In this paper, four widely spread algorithms are selected as an example for the proposed framework. They are APR [21], EMDD [40], Bag-SVM, and Inst-SVM [35], respectively.

1) **APR.** APR [21] is the first class of algorithms that were proposed to approach the MIL problem. It aims to find an axis-parallel hyperrectangle (APR) that contains at least one instance from every positive bag and no instances from any negative bag. This is achieved by starting with a point in the feature space and growing it to a minimum rectangle.
2) **EMDD.** The basic idea of EMDD [40] is to model the label of each bag with a hidden variable, which is estimated by the expectation–maximization (EM) algorithm. It combines the EM algorithm with the diverse density

(DD) algorithm [41], [42] to search for the maximum-likelihood hypothesis. It is defined as

$$h^* = \arg\max_h P(h\,|T) = \arg\min_h \sum_{i=1}^{b} (-\log\, P(\ell_i\,|h, B_i)) \quad (2)$$

where h is the concept space, and h^* is the concept point to be learned.

3) **Bag-SVM and Inst-SVM.** The SVM-based algorithm [35] is trying to maximize the soft margin between two types of bags or instances, which leads to Bag-SVM and Inst-SVM. It looks for a linear discriminant such that there is at least one instance from every positive bag in the positive half-space, whereas all instances belonging to negative bags are in the negative half-space. It follows the general prototype of SVM and is defined as

$$\min_{\mathrm{w},b,\xi} \frac{1}{2}\|\mathrm{w}\|^2 + C\sum_i \xi_i \quad \text{s.t.} \quad \forall i\ \ell_i \max_j(\langle \mathrm{w}, B_{ij}\rangle + b) \geq 1 - \xi_i. \quad (3)$$

C. Algorithm Overview

To learn the models by the aforementioned four algorithms, training data are constructed from 200 images with ground-truth delineation of salient objects. (The data set will be explained in detail in Section IV.) The training procedure is as follows. For each image, it is first segmented into distinct regions by a mean-shift algorithm [43], which are then treated as bags. Then, instances are randomly sampled from the bag. To keep the efficiency and feasibility, only 1% of the pixels within the bag are sparsely chosen as its instances. The bag will be labeled positive if there is at least one positive instance and negative if all instances are negative. After that, the parameters of the aforementioned four algorithms are trained on these labeled bags. For the testing stage, bags and instances are similarly obtained first. Then, the previous trained models are utilized to determine the saliency for each bag. To have a clear overview of the proposed algorithm, the pseudocode is listed in Algorithm 1.

Algorithm 1 Saliency Detection by MIL
Input:
Training images $I_i (i \in [1, 200])$.
Ground-truth saliency for each image.
Training Stage:
1:**for** each image $I_i (i \in [1, 200])$ in the training set **do**
2: Segment I_i by a mean-shift algorithm to get bags.
3: Sample instances within each bag.
4: Extract feature vector for each instance.
5:**end for**
6:Train the classifier with the feature vectors by APR, EMDD, Bag-SVM, and Inst-SVM.
Testing Stage:
1:**for** each image $I_j (j \in [1, 800])$ in the testing set **do**
2: Segment I_j by a mean-shift algorithm to get bags.
3: Sample instances within each bag.
4: Extract feature vector for each instance.
5: Calculate saliency of each bag according to the learned model.
6:**end for**
Output: detected saliency maps.

III. Image Features for Saliency Definition

The proposed framework for saliency detection have utilized low-, mid-, and high-level features. They are position, color, texture, scale, center prior, and boundary. Parameters with respect to these features are calibrated according to the training data. After obtaining all these features, a vector concatenating each feature output is formed to train and test the classifier by MIL.

A. Low-Level Feature

Position. The spatially connected pixels are prone to share similar saliency, whereas pixels far away tend to be differently salient. Therefore, the position of each instance is an essential factor for keeping the saliency consistent. Since the sizes of images differ, the absolute horizontal and vertical position is not suitable for an optimal feature. To avoid this problem, the normalized position within the range of [0, 1] is adopted to ensure that the measurement with respect to different images is comparable.

Color. This is the most frequently employed feature. Almost every algorithm for saliency detection will refer to it as the major supporting information for saliency calculation. However, for the choice of color spaces, there is not a non-controversial agreement. Some algorithms propose to use $L^*a^*b^*$ space because it is perceptually meaningful. Others claim the red, green, blue (RGB) space is more suitable for this task because it is computationally efficient. There is still no experimental justification for different choices. In this paper, three typical color spaces are respectively taken to calculate saliency. They are $L^*a^*b^*$, RGB, and hue, saturation, value (HSV). The one with the best performance will be chosen for this work. From the precision–recall curves (it will be explained in detail in Section IV) in Fig. 2, it is apparent that HSV color space performs the best. Accordingly, HSV is selected for this work.

With the most appropriate color space, color contrast is defined for each pixel, i.e.,

$$S_c(i, R_i) = \sum_{j \neq i,\, j \in R_i} d_c(i, j) \quad (4)$$

where i is the examined pixel, R_i is the supporting region for defining the saliency of pixel i, and $d_c(i, j)$ is the distance of color descriptors between i and j. The supporting region can be small as the 8-neighbors or as large as the whole image. However, a larger region may produce a more reliable result because it can exclude the influence of noise. As a result, it is set as the whole image in this work.

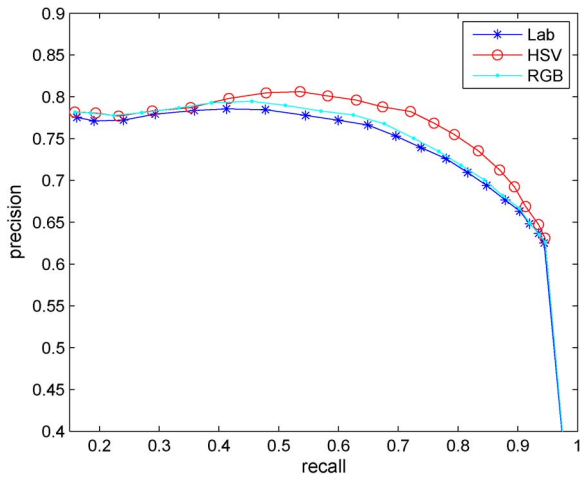

Fig. 2. Selection of color space. $L^*a^*b^*$, HSV, and RGB spaces are evaluated to choose a better one for saliency detection.

Texture. Different organizations of pixels form different textures, which would provide us with descriptively perceptual information. For saliency detection, this is also a significant feature. The perceived textures can be described by different ways but are generally characterized by the outputs of a set of filters. As an example, the filter bank used in this paper is made of copies of a Gaussian derivative and its Hilbert transform, which model the symmetric receptive fields of simple cells in visual cortex [44]. To be more specific, they are

$$f_1(x,y) = \frac{d^2}{dy^2}\left(\frac{1}{C}\exp\left(\frac{y^2}{\sigma^2}\right)\exp\left(\frac{x^2}{\ell^2\sigma^2}\right)\right)$$
$$f_2(x,y) = Hilbert\left(f_1(x,y)\right) \quad (5)$$

where σ is the scale, ℓ is the ratio of the filter, and C is a normalization constant. Similarly, texture contrast for each pixel is defined as

$$S_t(i,R_i) = \sum_{j\neq i,\, j\in R_i} d_t(i,j) \quad (6)$$

where R_i and $d_t(i,j)$ have an analogous meaning with color contrast. Since the texture descriptor is a continuous-valued vector, the problem of computational complexity exists, too. In order to be more efficient, a limited number of *textons* are trained from a set of images. Since textons are the prototype texture representations, the textures are quantized to k_t textons. Generally, k_t is set as 32, 64, or 128. However, experiments show that the selection of 128 is computationally infeasible, whereas 32 is too small to be distinguishable. Therefore, they are set to 64.

Scale. Scale is an effective property for identifying objects of different sizes. It is interpreted as a low-level feature in this paper. The approach taken to incorporate this feature follows [23]. To be more specific, the difference between fine and coarse scales of color images is extracted to simulate the center-surround operations of visual receptive fields. Such an architecture is particularly well suited to detecting the standing-out locations from their surroundings.

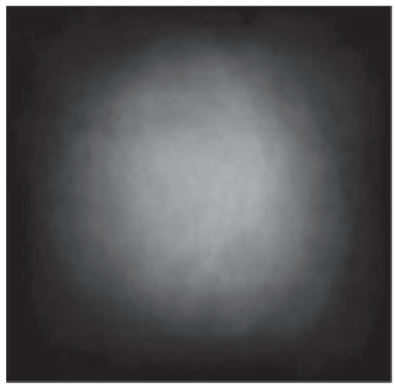

Fig. 3. Statistical map of saliency distribution on 200 training images. Each pixel in the map indicates the possibility of being salient for a normalized image with fixed size.

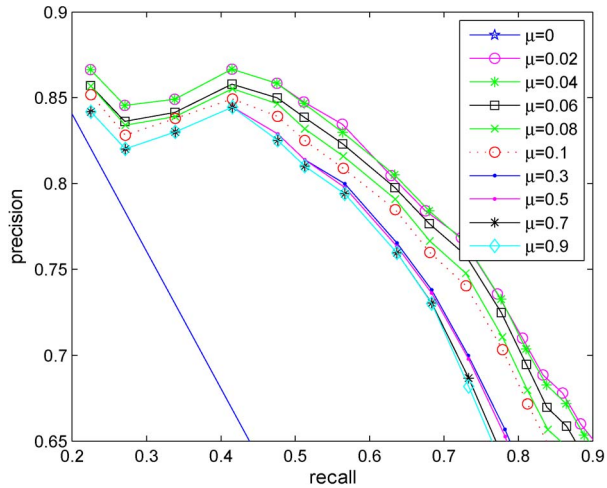

Fig. 4. Selection of parameter μ for center-prone prior. μ is varied from 0 to 1 in a 0.01 spacing to evaluate the performance.

B. Midlevel Feature

Center-prone prior. Several eye-tracking experiments have shown that people pay more attention to the center of an image. This rule is true for the 200 training images, as illustrated in Fig. 3. Han *et al.* [7] employed this principle in their algorithm. However, it is usually found that a salient object lies at the boundary of the image and the attention is not absolutely centered. In addition, even when the object is not at the boundary, the area might spread biasedly toward one direction. In this case, the center-weighting principle will fail. Inspired by the work of Cheng *et al.* [31], we adopt a principle that emphasizes more on the close supporting region and less on the far one for the examined region. In addition, regions with μ percentage of edge pixels on the image boundary will be punished to make its saliency set to 0.

To determine the optimal parameter of μ, experiments are done on the 200 training images. The possible parameter space is varied from 0 to 1 in a 0.01 spacing. For a better demonstration of the results, only part of the curves is illustrated in Fig. 4. It is manifest from the figure that $\mu = 0.04$ and $\mu = 0.02$ are the best choices. In this work, $\mu = 0.04$ is selected.

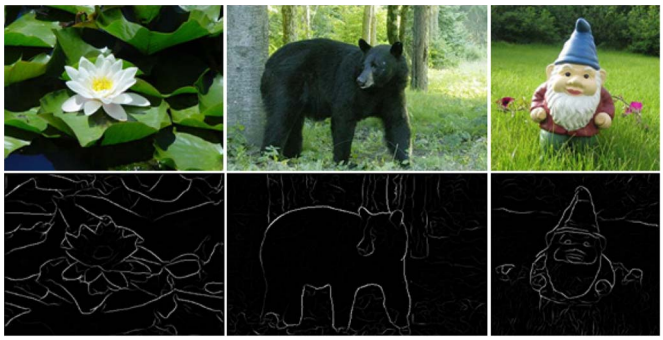

Fig. 5. Extracted boundary. The boundary is learned from a set of training images by a logistic model. Then, it is employed as a high-level feature.

C. High-Level Feature

Boundary. Saliency is related to human priors and perception. Low-level features can provide kinds of supporting information to determine the saliency level. However, we believe the involvement of a high-level feature is helpful for the delineation of salient objects. In this paper, we take boundary into consideration as an example for utilizing the high-level feature.

Boundary is different from what is traditionally known as edges. Edge is a low-level feature that indicates changes such as brightness, color, or texture. However, boundary implies the ownership from one object to another. Our assumption is that, if there is a boundary in a region, it is more possible to indicate a salient object within this region. Boundary is treated as an identifier to infer the salient objects.

To get the desired boundary, a learning-based approach [45] is used to train a logistic regression model, which integrates a set of image cues to output a probability boundary. Fig. 5 illustrates the boundary results.

IV. Evaluation

A. Data Set

In order to evaluate the performance of the proposed algorithms, a data set containing 1000 images is employed. It is constructed by Achanta *et al.* [16] and has achieved great popularity in saliency detection [31]. Every image in the data set has a ground-truth label. In this case, the experimental results can be evaluated quantitatively. Two hundred images are chosen for training purposes, and the remaining 800 are used for testing.

B. Evaluation Measure

In the experiments, the precision–recall measure [46], [47] is employed to evaluate the performance. It is a parametric curve that captures the tradeoff between accuracy and noise as the threshold varies. To get a better understanding of these two indexes, *true positives* (TP), *false positives* (FP), and *false negatives* (FN) should be first introduced.

For an information retrieval problem, suppose there are two classes—*positive* and *negative* (i.e., the salient objects and the other areas of an image in our application). *True positives* are the items that are correctly labeled as the positive class,

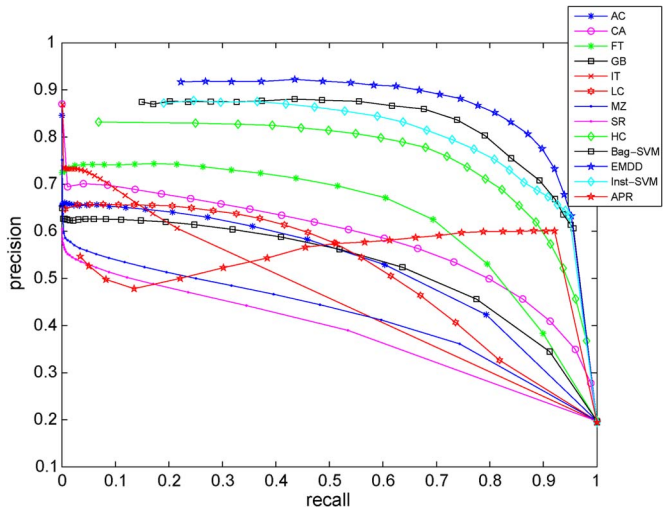

Fig. 6. Precision-recall curves of saliency detection results by different algorithms.

false positives are the ones incorrectly labeled as the positive class, and *false negatives* are the ones which are not labeled as the positive class but should have been. Based on these introductions, *precision* is defined as the rate of true positives divided by the whole labeled positive items (including true positives and false positives), whereas *recall* is defined as the rate of true positives divided by the actual number of items belonging to the positive class (including true positives and false negatives). In addition, F-measure, which is a weighted harmonic mean of precision and recall, is also taken to provide a single index. The three metrics are defined as

$$\begin{aligned} \text{precision} &= \frac{\text{TP}}{\text{TP}+\text{FP}} \qquad \text{recall} = \frac{\text{TP}}{\text{TP}+\text{FN}} \\ F\text{-measure} &= \frac{\text{precision} \times \text{recall}}{(1-\alpha) \times \text{precision} + \alpha \times \text{recall}} \end{aligned} \tag{7}$$

where α is set to 0.5 according to [45].

When thresholding the detected saliency result, it becomes a binary map. Varying the thresholds from small to big will lead to a series of binary maps, which correspond to a set of precision–recall values according to the ground-truth maps. Drawing these points on one figure will generate a precision–recall curve.

C. Performance

The results of the proposed algorithms are compared with nine popular algorithms, namely, AC [48], CA [15], FT [16], GB [30], IT [23], LC [33], MZ [49], SR [24], and HC [31]. The principle for selecting these algorithms is their recency, variety, and popularity. To be more specific, most of them are proposed in recent years or are cited many times and widely spread. In addition, they use different techniques to detect saliency, such as graph based, frequency tuned, MRF motivated, and context related. The codes for implementing these algorithms are from the authors' homepages or [31]. Every algorithm processes all of the 800 testing images, and the results are compared with the ground-truth labels to get a quantitative evaluation.

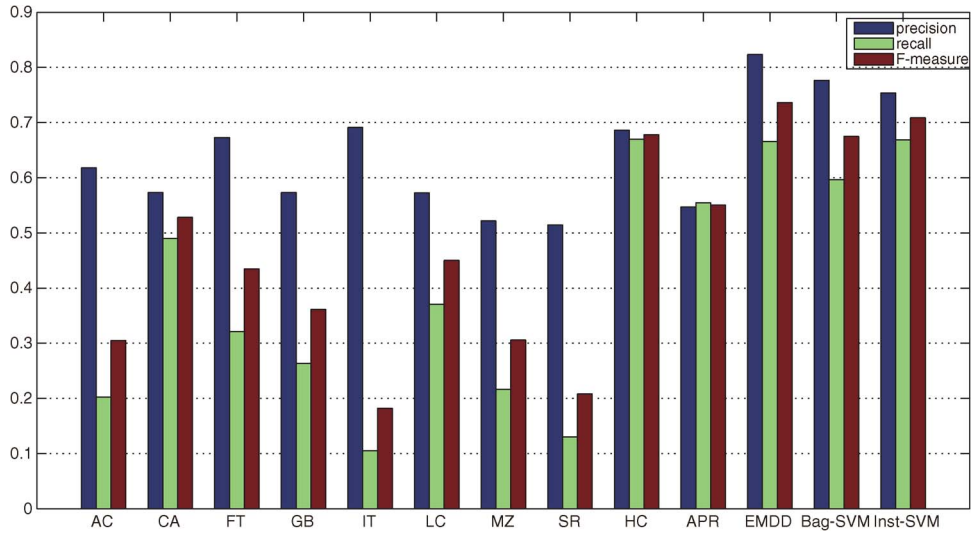

Fig. 7. Averaged precision, recall, and F-measure of saliency detection results by different algorithms.

Figs. 6 and 7 illustrate the results. The precision–recall curves and the averaged precision, recall, and F-measure bars are obvious to show that three of the proposed algorithms, i.e., EMDD, Bag-SVM, and Inst-SVM, outperform the other nine ones. Achieving the same precision value, the proposed algorithms can detect more salient regions; with the same recall value, the proposed algorithms are more accurate. Only APR does not perform very well, but its averaged recall and F-measure still outperform most other nine algorithms. This result is determined by the nature of the APR learning algorithm. For APR, its learning principle is simple, and the learned model generalizes poorly. It is achieved by increasing the size of an initially estimated hyperrectangle until every positive bag has at least one instance and every negative bag has no instance within it. In fact, there is an implicit assumption that the feature data can be classified by a hyperrectangle-like boundary. If the data distribution follows the underlying principle, a good result can be obtained. Otherwise, if the positive and negative data interlace with each other, a separating rectangle strictly dividing the data points into two sets is hard to find. Unfortunately, in this work, feature data are heavily interlaced. This makes the predicted results less accurate.

On the other hand, the SVM-based algorithm projects the original data into another space by a kernel mapping. At the same time, it maximizes the soft margin from the two types of positive and negative data. This makes the initially unclassified data possible to be classified. The EMDD algorithm converts multiple-instance data to single-instance data by removing all but one point per bag in the E-step. This cannot only reduce the computational time but also avoids getting caught in local minimum. The APR algorithm is the first formal algorithm for MIL, and it is not mature enough. Bag-SVM, Inst-SVM, and EMDD are all developed later than APR and aim to improve the performance of APR. Thus, it is natural to explain the experimental results.

As for the computational speed, APR and EMDD are much faster than Bag-SVM and Inst-SVM. On a computer with Intel Duo CPU of 2.93 GHz and 2-GB RAM, the former two may take tens of minutes, but the later two may take one or two days. Considering all these properties, EMDD is the best choice for this work because it has the best performance and fastest speed.

Several example results are also presented in Fig. 8 for qualitative evaluation. Only one of the four proposed algorithms, i.e., EMDD, is selected to compare with the other nine algorithms. These saliency maps in Fig. 8 are representative of the algorithms' performance. A careful investigation of the details of the produced maps would reveal that the proposed algorithm generates more consistent results than the other ones. The saliency of the target object is profoundly distinguished with the background. This is generally because the selective feature clues can be more distinguishable than other representations and the spatial constraint is more appropriate. Therefore, the proposed model can ensure that the target object stands out in a greater probability for each image.

D. Effects of Different Features

Here, effects of different features are evaluated to see whether its individual performance is better or its combination is more suitable. Low- and high-level features and their combination are first tested separately. Then, the midlevel feature, which is actually a spatial prior constraint, is integrated. The final results are averaged on the four presented algorithms and shown in Fig. 9. It is manifest that low- and high-level features do not perform well individually. The midlevel feature can improve their performance a lot. However, the best performance is achieved by employing all these features. The results are reasonable to explain because humans perceive the scene by integrated feature cues. A specific type of feature can only reflect an incomplete part of the information, whereas combining more image clues may make it more possible to understand the image content.

What deserves a further explanation of Fig. 9 is the fact that the detection results with the high-level feature perform worst in the experiments. This does not mean that the high-level feature is of less use. The reason is mainly that the high-level feature is hard to extract and utilize. Judd *et al.* [26]

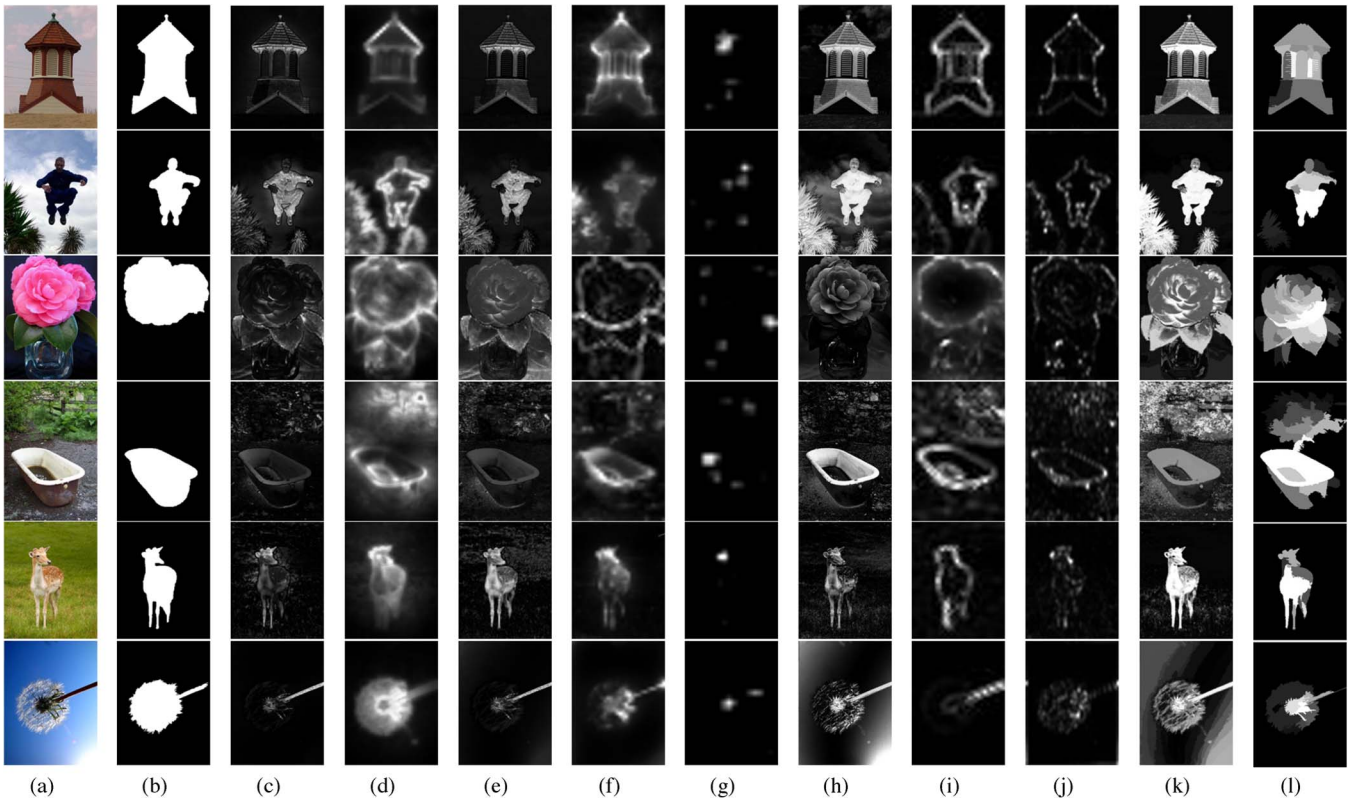

Fig. 8. (a) Original image. (b) Ground truth. Saliency maps produced by (c) AC [48], (d) CA [15], (e) FT [16], (f) GB [30], (g) IT [23], (h) LC [33], (i) MZ [49], (j) SR [24], (k) HC [31], and (l) the proposed EMDD in this paper.

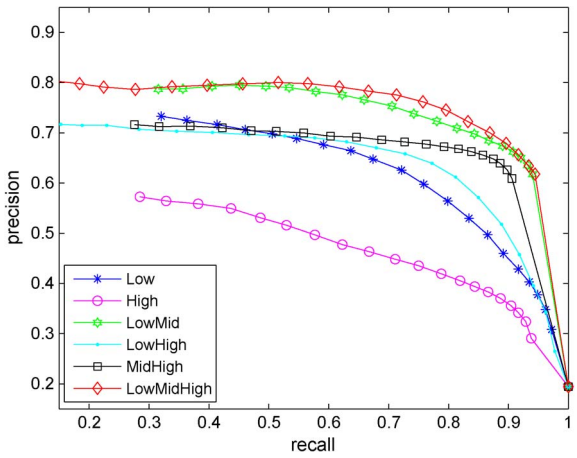

Fig. 9. Performance of saliency detection on different sets of features.

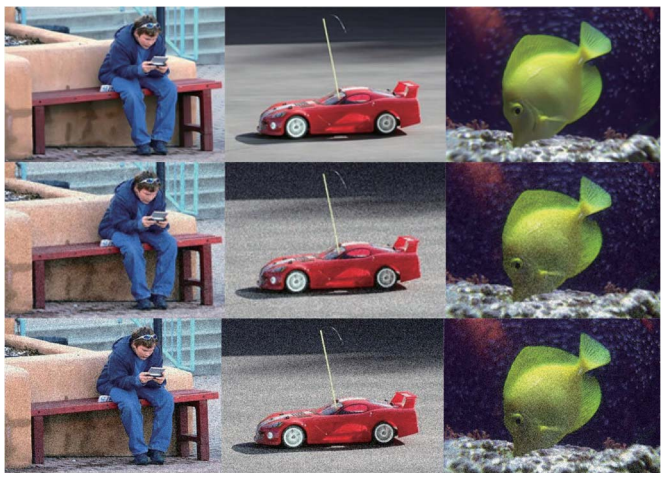

Fig. 10. Original images (first row) and its corresponding noisy images. Each image in the data set is added with white Gaussian noise, keeping SNR as 20 dB (second row) and 60 dB (third row).

incorporated face detection results into their algorithm as a high-level feature. This is lack of generality because not every image contains a face. Another option for employing a high-level feature is to involve human interaction. However, this is not practical for a large number of images. Therefore, in this paper, a learned boundary is adopted as a general high-level feature. The boundary feature is only effective to the bags with boundary pixels within them. We believe the high-level feature is most important for saliency detection. However, up to now, no perfect methodology is available to extract this information and how to use the feature (generally or application specifically) is far less mature. The work in this paper is just a meaningful attempt.

E. Robustness to Noise

A good algorithm cannot only achieve satisfying results for the testing data but also tolerate a certain level of noise. This property, which is regarded essential in this work, is not yet considered in existing work. In order to evaluate the robustness of saliency detection algorithms, white Gaussian noise is added to each testing image, keeping the SNR as 20 and 60 dB. Fig. 10 shows several example images with added noise. It is clear that each image is blurred by numerous dotlike flecks. However, the object–background content is still clear for us to identify.

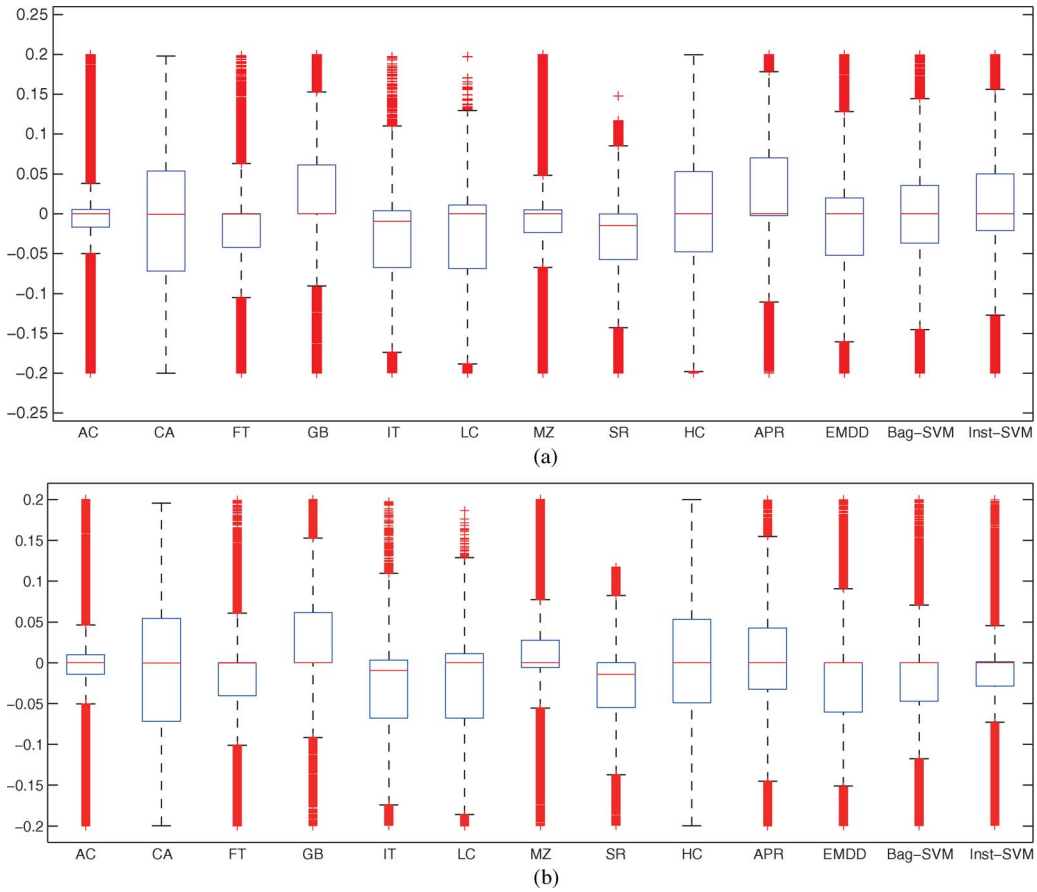

Fig. 11. Performance comparison before and after adding noise to images. The statistics reflect the algorithms' robustness to (a) 20-dB noise and (b) 60-dB noise.

Then, the averaged F-measure of each image before and after adding noise is compared to see the influence of the white Gaussian noise. Fig. 11 demonstrates the results with box graphs. The central mark of each box represents the median difference, the edges of the box are the 25th and 75th percentiles, the whiskers denote the most extreme data points, and outliers are plotted individually [50]. In both cases, the central red mark for each algorithm is around 0, with SR a little below zero level. This means that the averaged performance differences of the original and noised images are generally small. CA, LC, and HC have longer boxes, indicating a larger variance of their performance. AC, FT, and MZ have more outliers, implying the instability of these algorithms. GB and IT do not change much, but their visual results are not satisfying according to previous evaluation. For APR, EMDD, Bag-SVM, and Inst-SVM, their visual performance is promising. This can be justified from Section IV-C.

In both kinds of noise, although the sizes of the boxes vary with each other for these algorithms, their differences are below 0.05, which is not a big number. All these statistics together show that the presented algorithms and the nine existing ones have remarkable robustness to noise. However, the proposed algorithms have a better visual performance.

V. Image Retargeting Application

A good saliency model enables many applications that effectively take the attention of human perception into account. In order to comprehensively evaluate the proposed algorithms, the detected saliency map is further employed in an application of seam carving.

Seam carving [51], [52] is an important technique for content-based image resizing. A seam is defined as a connected path of pixels going from the top (left) of an image to the bottom (right). By removing seams from an image, the image is resized in the horizontal or vertical dimension. A successful algorithm would ensure that the target object in the image should not be disturbed.

In this work, seam carving is achieved by using an energy function defined on the pixels and removing minimum energy paths from the image [51], [52]. The saliency map is evaluated in the context of defining the energy function. Then, the seams with the minimum energy paths are removed according to a graph-cut framework. In the end, the image is resized to 75% the width of the original one, and the results are judged subjectively. By this means, the effectiveness of saliency detection can be evaluated. The HC algorithm [31], which has a comparable performance according to the precision–recall curves in Fig. 8, is chosen to be compared with the proposed EMDD algorithm. Fig. 12 shows the experimental results of seam carving. It is manifest that the saliency maps by the proposed algorithm are better than the HC maps, with a higher and consistent saliency degree in the target area. Therefore, the removed red seams in Fig. 12(d) and (g) are mainly from the background regions instead of disturbing the target ones.

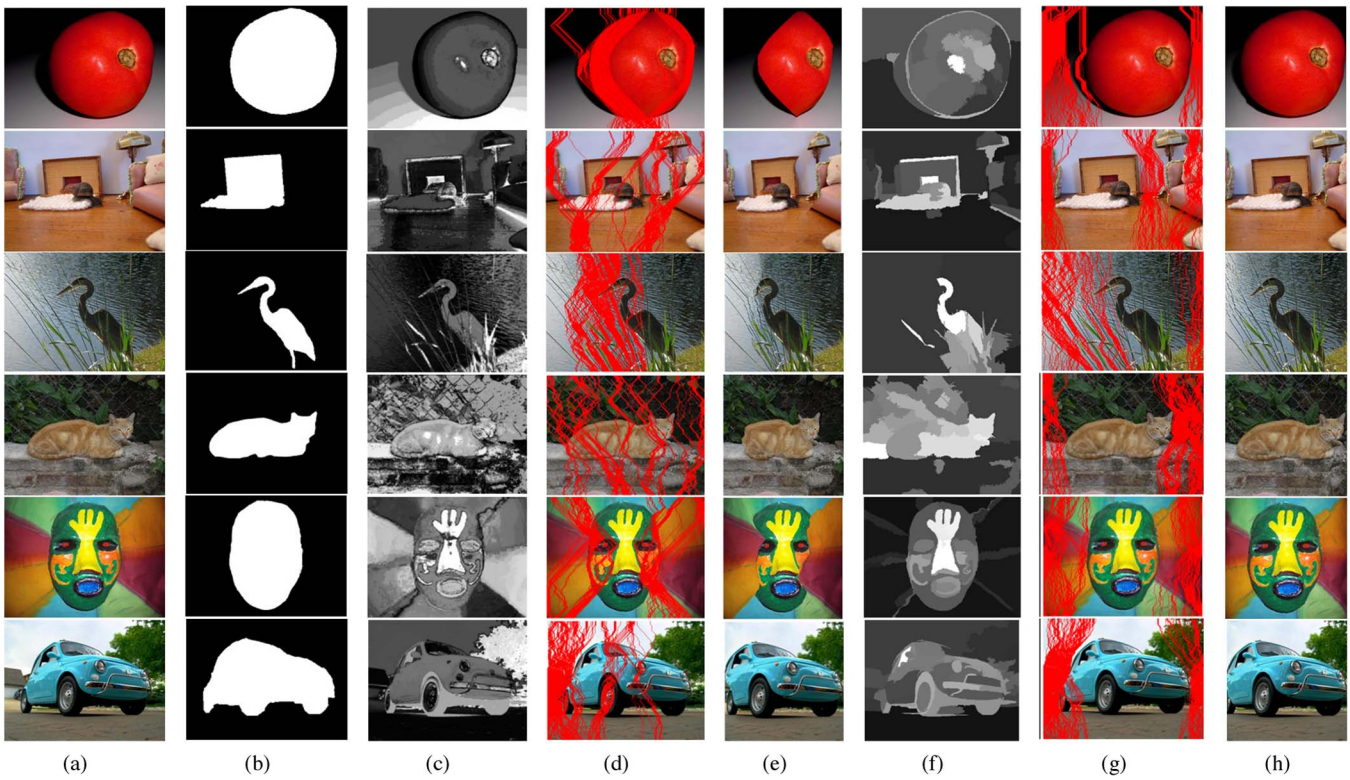

Fig. 12. (a) Original image. (b) Ground truth. (c) Saliency map by HC [31], (d) its corresponding carved seams, and (e) resized image. (f) Saliency map by the proposed algorithm EMDD, (g) its corresponding carved seams, and (h) resized image.

VI. Discussion

Here, several issues related to the proposed algorithm are discussed. The first issue is whether a principal component analysis (PCA) is needed to make the feature vector more compact. The second issue is about multiple salient object detection. The third issue is about parameter selection of a mean-shift segmentation algorithm. The fourth issue analyzes the results on images with rich textures. In the end, some negative results are shown and analyzed.

A. PCA on the Feature Vector

In the proposed algorithm, the feature vector is six dimensional, each component of which is horizontal position, vertical position, color contrast, texture contrast, scale contrast, and boundary identifier, respectively. Some argument may arise that PCA might be needed to make the feature vector more compact and optimal. To get a more appropriate representation, we have conducted a set of comparative experiments. The original feature vector is re-represented on six orthogonal eigenvectors by PCA. Then, we reduce the dimensionality from six to one. Fig. 13 shows the precision–recall results averaged by the four proposed algorithms on 800 testing images. From the curves, we can see that the 6-D PCA is close to the original representation. The other reduced representation performs worse. The worst performance is the 1-D feature vector. The reason behind this observation, we think, is that the original six features represent distinctive properties. There is no redundancy among them. Consequently, the reduced dimensionality results in a less distinguishable ability. Based on these experimental results, it is clear that the optimal feature representation is the original 6-D vector.

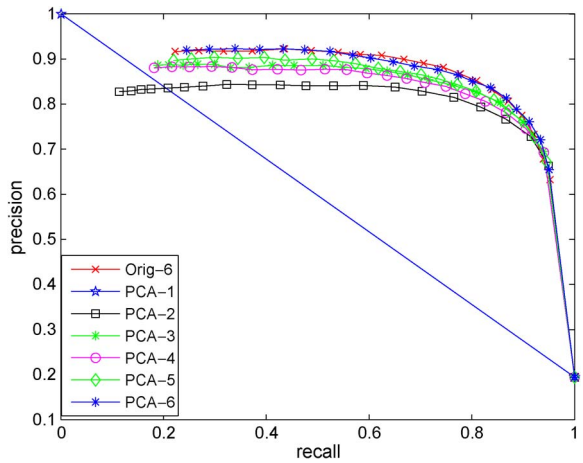

Fig. 13. Performance comparison using feature representations of different dimensionalities.

B. Multiple Object Detection

For an image, there may be more than one salient object. Our processing does not identify the number of salient objects in the examined image, which we think is another different topic from what is discussed in this paper. We just detect the salient areas for an input image, no matter if it contains one or several objects. Therefore, if there are multiple salient objects, the proposed algorithms can detect them, even when occlusions exist among objects. Many such examples abound in the employed data set. Fig. 14 demonstrates some typical examples.

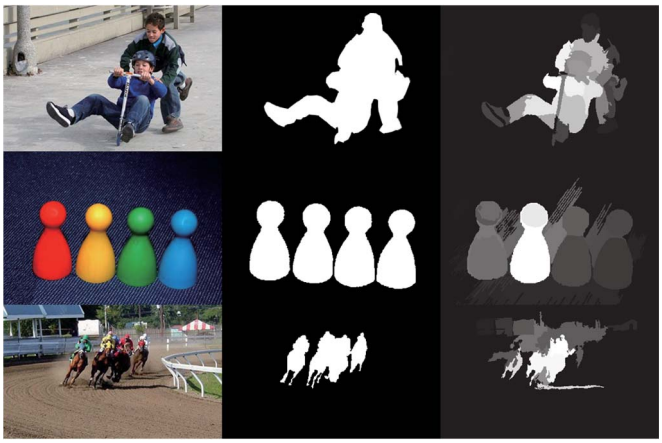

Fig. 14. Illustrative detection of multiple salient objects. (First column) Original images. (Second column) Ground-truth saliency results. (Third column) Saliency detection results by the proposed EMDD algorithm.

C. Selection of the Segmentation Parameter

The calculation of the proposed saliency detection algorithm is based on segmented regions. Therefore, the final results are influenced by the segmentation outputs. Too small regions will lead to an inconsistent result, and too large regions will result in an enlarged salient area. A proper choice of the segmentation parameter is the insurance of a good saliency detection result. There are three parameters for the employed mean-shift segmentation algorithm, namely, spatial bandwidth, color bandwidth, and minimum region. The default parameters are 7, 6.5, and 20, with which we find the saliency detection results are not satisfying. Empirical experiments show that a combination of 15, 10.5, and 500 is more appropriate. Throughout this paper, the segmentation is all conducted under this parameter set.

D. Results on Images With Rich Textures

For images with simple or no textures, the detected saliency results are mostly close to the ground-truth labels. For images with rich textures, satisfying results can be also obtained because our training data set contains images with different colors, textures, and contents. The learned model can tackle a variety of testing images. Fig. 15 illustrates some typical examples for rich-textured images.

E. Analysis of Negative Results

Here, several negative experimental results are demonstrated and analyzed. It is shown in Fig. 16 that the obtained results by the proposed algorithm are not satisfying compared with the ground-truth saliency results. We think there are three reasons for this problem. First, the segmentation results are not consistent with the human perception. Since the proposed algorithm calculates saliency on regions, which are acquired through segmentation, the segmentation results are highly correlated to the saliency calculation. Unfortunately, the state of the art for segmentation algorithms has not reached a level comparable with human perception. This will result in a segmented object

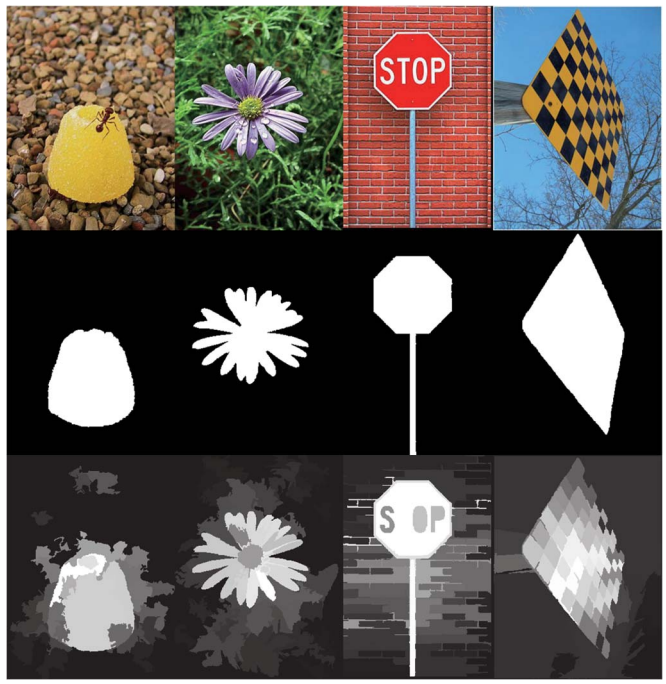

Fig. 15. Sample experimental results on images with rich textures. (First row) Original images. (Second row) Ground-truth saliency results. (Third row) Saliency detection results by the proposed EMDD algorithm.

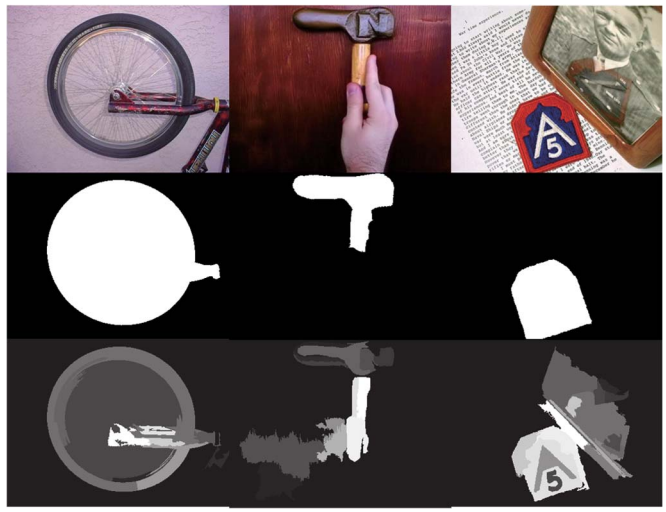

Fig. 16. Illustration of several negative results.

splitting into several parts. The first column in Fig. 16 is a typical example of this case. The wheel in the image is segmented as several parts, leading to an inconsistent detection result. Second, without appropriate higher level clues, the detected saliency can hardly reflect human's experience. This can be illustrated in the second column in Fig. 16. People will generally pay more attention to the object held in hand, rather than the hand itself. However, the computer cannot handle this situation. Although the boundary clue is incorporated in our processing, it is far from perfect to reflect a complete human experience. Third, the content of the image is sometimes ambiguous itself. In the third column in Fig. 16, it is difficult to tell which is more salient between the badge and the picture frame.

VII. Conclusion

In this paper, a supervised framework for saliency detection has been presented. The framework combines a set of low-, mid-, and high-level features to predict the possibilities of each region being salient. The approach it takes is MIL, and four implementations of MIL are demonstrated. To validate effectiveness and robustness, nine algorithms representing the state of the art are employed to be compared with the proposed algorithm. Experiments on a set of 1000 images show that the MIL-based algorithm outperforms the others. An application of seam carving is also involved to exemplify the usefulness of the proposed framework.

There are several remaining issues for further investigation. The first issue is how to extract more effective high-level features to be effectively incorporated into the detection framework. We believe that this might be the key point for tremendously improving the state of the art. The second issue is how to apply the saliency detection technique to specific applications.

References

[1] W. James, *The Principles of Psychology*. New York: Henry Holt, 1890.

[2] Y. Yu, G. K. I. Mann, and R. G. Gosine, "An object-based visual attention model for robotic applications," *IEEE Trans. Syst., Man, Cybern. B, Cybern.*, vol. 40, no. 5, pp. 1398–1412, Oct. 2010.

[3] K. Huang, D. Tao, Y. Y. Tang, X. Li, and T. Tan, "Biologically inspired features for scene classification in video surveillance," *IEEE Trans. Syst., Man, Cybern. B, Cybern.*, vol. 41, no. 1, pp. 307–313, Feb. 2011.

[4] Y. Huang, K. Huang, D. Tao, T. Tan, and X. Li, "Enhanced biologically inspired model for object recognition," *IEEE Trans. Syst., Man, Cybern. B, Cybern.*, vol. 41, no. 6, pp. 1668–1680, Dec. 2011.

[5] A. Oikonomopoulos, I. Patras, and M. Pantic, "Spatiotemporal salient points for visual recognition of human actions," *IEEE Trans. Syst., Man, Cybern. B, Cybern.*, vol. 36, no. 3, pp. 710–719, Jun. 2005.

[6] D. Walther, L. Itti, M. Riesenhuber, T. Poggio, and C. Koch, "Attentional selection for object recognition a gentle way," in *Proc. Biol. Motivated Comput. Vis.*, 2002, pp. 472–479.

[7] J. Han, K. N. Ngan, M. Li, and H. Zhang, "Unsupervised extraction of visual attention objects in color images," *IEEE Trans. Circuits Syst. Video Technol.*, vol. 16, no. 1, pp. 141–145, Jan. 2006.

[8] B. C. Ko and J.-Y. Nam, "Object-of-interest image segmentation based on human attention and semantic region clustering," *J. Opt. Soc. Amer. A, Opt. Image Sci.*, vol. 23, no. 10, pp. 2462–2470, Oct. 2006.

[9] Y.-S. Wang, C.-L. Tai, O. Sorkine, and T.-Y. Lee, "Optimized scale-and-stretch for image resizing," *ACM Trans. Graph.*, vol. 27, no. 5, pp. 1–8, Dec. 2008.

[10] T. Chen, M.-M. Cheng, P. Tan, A. Shamir, and S.-M. Hu, "Sketch2photo: Internet image montage," *ACM Trans. Graph.*, vol. 28, no. 5, pp. 1–10, Dec. 2009.

[11] L. Chen, X. Xie, X. Fan, W.-Y. Ma, H.-J. Zhang, and H. Zhou, "A visual attention model for adapting images on small displays," Microsoft Res., Redmond, MA, Tech. Rep. MSR-TR-2002-125, 2002.

[12] L. Itti, "Models of bottom-up and top-down visual attention," Ph.D. dissertation, California Inst. Technol., Pasadena, CA, 2000.

[13] X. Gao, N. Liu, W. Lu, D. Tao, and X. Li, "Spatio-temporal salience based video quality assessment," in *Proc. IEEE Int. Conf. Syst. Man Cybern.*, 2010, pp. 1501–1505.

[14] X. Li, S. Lin, S. Yan, and D. Xu, "Discriminant locally linear embedding with high-order tensor data," *IEEE Trans. Syst., Man, Cybern. B, Cybern.*, vol. 38, no. 2, pp. 342–352, Apr. 2008.

[15] S. Goferman, L. Zelnik-Manor, and A. Tal, "Context-aware saliency detection," in *Proc. IEEE Int. Conf. Comput. Vis. Pattern Recognit.*, 2010, pp. 2376–2383.

[16] R. Achanta, S. Hemami, F. Estrada, and S. Susstrunk, "Frequency-tuned salient region detection," in *Proc. IEEE Int. Conf. Comput. Vis. Pattern Recognit.*, 2009, pp. 1597–1604.

[17] K.-Y. Chang, T.-L. Liu, and S.-H. Lai, "From co-saliency to co-segmentation: An efficient and fully unsupervised energy minimization model," in *Proc. IEEE Int. Conf. Comput. Vis. Pattern Recognit.*, 2011, pp. 2129–2136.

[18] J. M. Wolfe and T. S. Horowitz, "What attributes guide the deployment of visual attention and how do they do it," *Nature Rev. Neurosci.*, vol. 5, no. 6, pp. 495–501, Jun. 2004.

[19] A. Treisman and G. Gelade, "A feature-integration theory of attention," *Cogn. Psychol.*, vol. 12, no. 1, pp. 97–136, Jan. 1980.

[20] R. Desimone and J. Duncan, "Neural mechanisms of selective visual attention," *Annu. Rev. Neurosci.*, vol. 18, no. 1, pp. 193–222, Mar. 1995.

[21] T. G. Dietterich, R. H. Lathrop, and T. Lozano-Pérez, "Solving the multiple instance problem with axis-parallel rectangles," *Artif. Intell.*, vol. 89, no. 1/2, pp. 31–71, Jan. 1997.

[22] C. Koch and S. Ullman, "Shifts in selective visual attention: Towards the underlying neural circuitry," *Hum. Neurobiol.*, vol. 4, no. 4, pp. 219–227, 1985.

[23] L. Itti, C. Koch, and E. Niebur, "A model of saliency-based visual attention for rapid scene analysis," *IEEE Trans. Pattern Anal. Mach. Intell.*, vol. 20, no. 11, pp. 1254–1259, Nov. 1998.

[24] X. Hou and L. Zhang, "Saliency detection: A spectral residual approach," in *Proc. IEEE Int. Conf. Comput. Vis. Pattern Recognit.*, 2007, pp. 1–8.

[25] T. Liu, J. Sun, N. Zheng, X. Tang, and H.-Y. Shum, "Learning to detect a salient object," in *Proc. IEEE Int. Conf. Comput. Vis. Pattern Recognit.*, 2007, pp. 1–8.

[26] T. Judd, K. A. Ehinger, F. Durand, and A. Torralba, "Learning to predict where humans look," in *Proc. Int. Conf. Comput. Vis.*, 2009, pp. 2106–2113.

[27] Z. Wang and B. Li, "A two-stage approach to saliency detection in images," in *Proc. IEEE Int. Conf. Acoust., Speech, Signal Process.*, 2008, pp. 965–968.

[28] A. Radhakrishna and S. Sabine, "Saliency detection using maximum symmetric surround," in *Proc. IEEE Int. Conf. Image Process.*, 2010, pp. 2653–2656.

[29] L. Zhang, M. H. Tong, T. K. Marks, H. Shan, and G. W. Cottrell, "Sun: A Bayesian framework for saliency using natural statistics," *J. Vis.*, vol. 8, no. 7, pp. 1–20, Dec. 2008.

[30] J. Harel and P. P. C. Koch, "Graph-based visual saliency," in *Proc. Adv. Neural Inf. Process. Syst.*, 2006, pp. 545–552.

[31] M.-M. Cheng, G.-X. Zhang, N. J. Mitra, X. Huang, and S.-M. Hu, "Global contrast based salient region detection," in *Proc. IEEE Int. Conf. Comput. Vis. Pattern Recognit.*, 2011, pp. 409–416.

[32] M. Wang, J. Konrad, P. Ishwar, K. Jing, and H. A. Rowley, "Image saliency: From intrinsic to extrinsic context," in *Proc. IEEE Int. Conf. Comput. Vis. Pattern Recognit.*, 2011, pp. 417–424.

[33] Y. Zhai and M. Shah, "Visual attention detection in video sequences using spatiotemporal cues," *Proc. ACM Multimedia*, pp. 815–824, 2006.

[34] T. Liu, Z. Yuan, J. Sun, J. Wang, N. Zheng, X. Tang, and H.-Y. Shum, "Learning to detect a salient object," *IEEE Trans. Pattern Anal. Mach. Intell.*, vol. 33, no. 2, pp. 353–367, Feb. 2011.

[35] S. Andrews, I. Tsochantaridis, and T. Hofmann, "Support vector machines for multiple-instance learning," *Proc. Adv. Neural Inf. Process. Syst.*, pp. 561–568, 2002.

[36] J. Wang and J.-D. Zucker, "Solving the multiple-instance problem: A lazy learning approach," in *Proc. Int. Conf. Mach. Learn.*, 2000, pp. 1119–1126.

[37] R. A. Amar, D. R. Dooly, S. A. Goldman, and Q. Zhang, "Multiple-instance learning of real-valued data," in *Proc. Int. Conf. Mach. Learn.*, 2001, pp. 3–10.

[38] P. A. Viola, J. C. Platt, and C. Zhang, "Multiple instance boosting for object detection," in *Proc. Adv. Neural Inf. Process. Syst.*, 2005, pp. 1417–1426.

[39] B. Babenko, M.-H. Yang, and S. Belongie, "Robust object tracking with online multiple instance learning," *IEEE Trans. Pattern Anal. Mach. Intell.*, vol. 33, no. 8, pp. 1619–1632, Aug. 2011.

[40] Q. Zhang and S. A. Goldman, "EM-DD: An improved multiple-instance learning technique," in *Proc. Adv. Neural Inf. Process. Syst.*, 2001, pp. 1073–1080.

[41] O. Maron and T. Lozano-Pérez, "A framework for multiple-instance learning," in *Proc. Adv. Neural Inf. Process. Syst.*, 1997, pp. 570–576.

[42] O. Maron and A. L. Ratan, "Multiple-instance learning for natural scene classification," in *Proc. Int. Conf. Mach. Learn.*, 1998, pp. 341–349.

[43] D. Comaniciu and P. Meer, "Mean shift: A robust approach toward feature space analysis," *IEEE Trans. Pattern Anal. Mach. Intell.*, vol. 24, no. 5, pp. 603–619, May 2002.

[44] J. Malik, S. Belongie, T. K. Leung, and J. Shi, "Contour and texture analysis for image segmentation," *Int. J. Comput. Vis.*, vol. 43, no. 1, pp. 7–27, Jun. 2001.

[45] D. R. Martin, C. Fowlkes, and J. Malik, "Learning to detect natural image boundaries using local brightness, color, and texture cues," *IEEE Trans. Pattern Anal. Mach. Intell.*, vol. 26, no. 5, pp. 530–549, May 2004.
[46] D. L. Olson and D. Delen, *Advanced Data Mining Techniques*. Berlin, Germany: Springer-Verlag, Mar. 4, 2008.
[47] [Online]. Available: http://en.wikipedia.org/wiki/Precision_and_recall
[48] R. Achanta, F. J. Estrada, P. Wils, and S. Süsstrunk, "Salient region detection and segmentation," in *Proc. Comput. Vis. Syst.*, 2008, pp. 66–75.
[49] Y.-F. Ma and H. Zhang, "Contrast-based image attention analysis by using fuzzy growing," in *Proc. ACM Multimedia*, 2003, pp. 374–381.
[50] [Online]. Available: www.mathworks.cn/help/toolbox/stats/boxplot.html
[51] S. Avidan and A. Shamir, "Seam carving for content-aware image resizing," *ACM Trans. Graph.*, vol. 26, no. 3, pp. 1–10, Jul. 2007.
[52] M. Rubinstein, A. Shamir, and S. Avidan, "Improved seam carving for video retargeting," *ACM Trans. Graph.*, vol. 27, no. 3, pp. 1–9, Aug. 2008.

Qi Wang received the B.E. degree in automation and the Ph.D. degree in pattern recognition and intelligent system from the University of Science and Technology of China, Hefei, China, in 2005 and 2010, respectively.

He is currently a Postdoctoral Researcher with the Center for Optical Imagery Analysis and Learning, State Key Laboratory of Transient Optics and Photonics, Xi'an Institute of Optics and Precision Mechanics, Chinese Academy of Sciences, Xi'an, China. His research interests include computer vision and pattern recognition.

Yuan Yuan (M'05–SM'09) is currently a Researcher and Full Professor with the Chinese Academy of Sciences, Xi'an, China. Her main research interests include visual information processing and image/video content analysis.

Pingkun Yan (S'04–M'06–SM'10) received the B.Eng. degree in electronics engineering and information science from the University of Science and Technology of China, Hefei, China, and the Ph.D. degree in electrical and computer engineering from the National University of Singapore, Singapore.

He is currently a Full Professor with the Center for OPTical IMagery Analysis and Learning (OPTIMAL), State Key Laboratory of Transient Optics and Photonics, Xi'an Institute of Optics and Precision Mechanics, Chinese Academy of Sciences, Xi'an, China. His research interests include computer vision, pattern recognition, machine learning, and their applications in medical imaging.

Xuelong Li (M'02–SM'07–F'12) is currently a Full Professor with the Center for OPTical IMagery Analysis and Learning (OPTIMAL), State Key Laboratory of Transient Optics and Photonics, Xi'an Institute of Optics and Precision Mechanics, Chinese Academy of Sciences, Xi'an, China.